^{18}F-FDG PET Studies in Patients with Extratemporal and Temporal Epilepsy: Evaluation of an Observer-Independent Analysis

Alexander Drzezga, Stephan Arnold, Satoshi Minoshima, Soheyl Noachtar, Johann Szecsi, Peter Winkler, Wolfgang Römer, Klaus Tatsch, Wolfgang Weber and Peter Bartenstein

Department of Nuclear Medicine, Technische Universität, München; Departments of Neurology, Neurosurgery and Nuclear Medicine, Ludwig-Maximilians-Universtät, München, Germany; Division of Nuclear Medicine, Department of Internal Medicine, University of Michigan, Ann Arbor, Michigan

The aim of this study was to evaluate an observer-independent analysis of ^{18}F-fluorodeoxyglucose (FDG) PET studies in patients with temporal or extratemporal epilepsy. **Methods:** Twenty-seven patients with temporal epilepsy and 22 patients with extratemporal epilepsy were included in the study. All patients with temporal epilepsy and 7 patients with extratemporal epilepsy underwent surgical treatment. In patients who showed significant postoperative improvement (temporal, n = 23; extratemporal, n = 6), the epileptogenic focus was assumed to be located in the area of surgical resection. In extratemporal epilepsy patients who did not undergo surgery, the focus localization was determined using a combination of semiology, ictal and interictal electroencephalography, [^{99m}Tc]ethyl cysteinate dimer SPECT, MRI and [^{11}C]flumazenil PET. Visual analysis was performed by two experienced and two less experienced blinded observers using sagittal, axial and coronal images. In the automated analysis after anatomic standardization and generation of three-dimensional stereotactic surface projections (SSPs), a pixelwise comparison of ^{18}F-FDG uptake with an age-matched reference database (n = 20) was performed, resulting in *z* score images. Pixels with the maximum deviation were detected, summarized and attached to one of 20 predefined surface regions of interest. For comparison with ^{18}F-FDG PET and MR images, three-dimensional overlay images were generated. **Results:** In patients with temporal epilepsy, the sensitivity was comparable for visual and observer-independent analysis (three-dimensional SSP 86%, experienced observers 86%–90%, less experienced observers 77%–86%). In patients with extratemporal epilepsy, three-dimensional SSP showed a significantly higher sensitivity in detecting the epileptogenic focus (67%) than did visual analysis (experienced 33%–38%, each less experienced 19%). In temporal lobe epilepsy, there was moderate to good agreement between the localization found with three-dimensional SSP and the different observers. In patients with extratemporal epilepsy, there was a high interobserver variability and only a weak agreement between the localization found with three-dimensional SSP and the different observers. Although three-dimensional SSP detected multiple lesions more often than visual analysis, the determination of the highest deviation from the reference database allowed the identification of the epileptogenic focus with a higher accuracy than subjective criteria, especially in extratemporal epilepsy. **Conclusion:** Three-dimensional SSP increases sensitivity and reduces observer variability of the analysis of ^{18}F-FDG PET images in patients with extratemporal epilepsy and is, therefore, a useful tool in the evaluation of this patient group. The benefit of this analytical approach in patients with temporal epilepsy is less apparent.

Key Words: extratemporal; epilepsy; ^{18}F-fluorodeoxyglucose; PET; computer-assisted image processing

J Nucl Med 1999; 40:737–746

It has been known for almost two decades that epileptogenic foci induce a reduction of interictal glucose metabolism (*1*). PET studies using ^{18}F-fluorodeoxyglucose (FDG) have been performed in epileptic patients to detect and localize epileptogenic foci. Numerous studies, some of which consisted of large numbers of patients, have reported a sensitivity of 70%–85% for ^{18}F-FDG PET in patients with temporal epilepsy (*2–4*). In extratemporal epilepsy, however, the patient populations investigated were smaller, and the values for diagnostic sensitivity and accuracy reported for interictal studies were significantly lower: 45% or less depending on the localization of the focus (*3,5,6*). It is unclear to what extent this significantly lower diagnostic accuracy in patients with extratemporal epilepsy is caused by the lower sensitivity of the method itself or by a higher dependency of the visual interpretation of the PET images on the experience of the observer (*7,8*). The variability in the localization of the epileptogenic lesion, the high incidence of multiple lesions and the greater variability of interaction between epileptogenic tissue and functionally associated cortical regions, compared with temporal foci (*5,9–12*), make visual assessment of the PET images in this patient population more difficult. Furthermore, localization with extra- and intracranial electroencephalography (EEG) has also been shown to be unreliable in patients with extratemporal epilepsy (*9,13*).

The poor diagnostic accuracy of PET and other diagnostic

Received May 26, 1998; revision accepted Oct. 7, 1998.

For correspondence or reprints contact: Alexander Drzezga, MD, Nuklearmedizinische, Klinik und Poliklinik, der Technischen Universität München, Klinikum rechts der Isar, Ismaninger Str. 22, 81675 München, Germany.

modalities may explain why few patients with extratemporal epilepsy receive surgical treatment and why postoperative results are often unsatisfactory. After temporal lobe resection, approximately 70% of patients with refractory temporal epilepsy become seizure free, whereas an average of approximately 45% of patients with extratemporal epilepsy were reported to be seizure free postoperatively (*4*). The unsuccessful surgeries may be caused in part by indeterminate localization and, in particular, the extent of the epileptogenic lesion, even when combining results from EEG, MRI and functional imaging (*14*). Therefore, increasing the diagnostic accuracy of interictal ^{18}F-FDG PET may improve these poor therapeutic results.

Thus, the aim of this study was to evaluate the usefulness of an observer-independent approach (initially designed for the investigation of dementing disorders [*15*]) to identify and localize a seizure focus in ^{18}F-FDG images in comparison with visual assessment in patients with temporal or extratemporal epilepsy.

MATERIALS AND METHODS

Patient Characteristics

A total of 27 patients with temporal epilepsy (18 women, 9 men; mean age 37 ± 9 y) and 22 patients with extratemporal epilepsy (9 women,13 men; mean age 27 ± 9 y) who underwent a routine PET investigation with ^{18}F-FDG as part of their presurgical diagnostic program were included in this study. The mean duration of the disease for the temporal and extratemporal epilepsy groups was 29 ± 6 y and 20 ± 4 y, respectively. All patients had focal seizures (classified according to a new seizure and EEG classification by Luders and Noachtar [*16,17*]), and 81% of the patients had experienced occasional secondary generalization (19 of the patients with extratemporal and 21 of the patients with temporal epilepsy). All patients were integrated into a presurgical diagnostic program for possible surgical treatment because of unsuccessful antiepileptic drug therapy. Only patients who had epilepsy surgery or who showed a single epileptogenic focus defined by noninvasive means were included in the study.

All 27 patients with temporal epilepsy and 7 patients with extratemporal epilepsy underwent surgical intervention. The resected specimens were analyzed histopathologically. Postoperative outcome was rated using a classification introduced by Engel (*18*). It consists of four classes, each containing several subgroups: class I, free of disabling seizures; class II, rare disabling seizures; class III, worthwhile improvement; class IV, no worthwhile improvement.

In all patients who had successful resection (Engel class I or II), the area of resection was assumed to be the localization of the epileptogenic focus. Patients without significant postoperative improvement were not included in the sensitivity analysis. For patients who did not undergo surgery (15 patients with extratemporal epilepsy), the focus was defined by a combination of seizure-semiology, ictal and interictal EEG, MRI, ictal [^{99m}Tc]ethyl cysteinate dimer (ECD) SPECT imaging and [^{11}C]flumazenil (FMZ) PET. For the purpose of this study, localization of the epileptogenic focus required that ictal surface EEG semiology correspond with at least one additional method (invasive EEG recording, MRI, [^{11}C]FMZ PET or ictal [^{99m}Tc]ECD SPECT). Because MRI was performed in all patients, ictal [^{99m}Tc]ECD SPECT or [^{11}C]FMZ PET was used for focus localization if MRI showed no abnormalities or ambiguous abnormalities. Patients who did not fulfill these criteria were not included in the study.

For patients who underwent surgery, the cause of the epilepsy was defined by postoperative histopathologic analysis of the resected brain tissue. In the remaining patients, a synopsis of history, semiology and MRI findings was used to define the probable cause.

^{18}F-FDG PET Imaging Technique

PET scans were obtained in the interictal state with ^{18}F-FDG under standard resting conditions (eyes closed in dimmed ambient light) using a Siemens 951 R/31 PET scanner (CTI, Knoxville, TN). Acquisitions were in two-dimensional mode with a total axial field of view of 10.5 cm and no interplane dead space. To obtain transaxial images approximately parallel to the intercommisural line (AC-PC line), patients were positioned with the canthomeatal line parallel to the detector rings. For attenuation correction, a transmission scan was obtained with an external ^{68}Ge ring source before tracer injection. Thirty minutes after injection of 370 MBq ^{18}F-FDG, a sequence of three 10-min frames was started and later combined into a single frame.

Image Analysis

Image analysis was performed on a Sun workstation (Sun Microsystems, Inc., Mountain View, CA). Automated analysis of the ^{18}F-FDG PET images was performed using a modification of a program that generates standardized three-dimensional stereotactic surface projections (SSPs) of the individual dataset followed by a pixelwise comparison with a normal database resulting in *z* score images. This routine has been described previously and evaluated in patients with dementing disorders (*8,15,19–22*).

The most important steps of the program are described below: The initial step included a rotational correction and centering of the dataset in three dimensions, resulting in a realignment of the AC-PC line (*19*). To adjust the individual's brain to the proportional grid system proposed by Talairach and Tournoux (*23*), linear scaling and nonlinear warping of the data were performed, resulting in a standardized image set with a uniform voxel size of 2.25 mm (*20*).

Three-dimensional SSPs were generated to visualize cortical gray matter activity (*15*). In this approach, the maximum pixel values on predefined vectors perpendicular to the surface and covering the entire standardized outer brain contour were determined with a search depth of 6 pixels (13.5 mm). The detected maximum pixel values were then assigned to the corresponding surface pixel of the standardized surface. The resulting three-dimensional SSP images allowed the visualization of all aspects of the brain surface (*15*).

The thalamus was chosen as the most robust reference region for the subsequent analysis of the patient data. Because regional temporal or extratemporal hypometabolism can affect the metabolic activity of the ipsilateral thalamus (*24*), the side containing the higher average value was selected for normalization. (*8,15*).

Comparison of the normalized brain activity of each patient with a reference normal database consisting of 20 age-matched normal controls was performed by means of a *z* score (*15*). *Z* scores were calculated pixelwise on the three-dimensional-SSP format. A high, local *z* score represents reduced local glucose metabolism relative to the control mean. To allow visualization, *z* scores were projected on surface views in the same manner as the three-dimensional SSP images.

To minimize interobserver variability in determining the location of the most significant hypometabolic zone, further steps were added to the analysis: A predefined set of 20 surface regions of interest (ROIs) was placed automatically onto the three-dimensional SSP z score images (Fig. 1). The ROIs were defined to reflect the known functional divisions of the cerebral lobes (*25*), and each hemisphere was divided into the following regions: orbitofrontal, prefrontal, premotor, central, parietal superior and inferior, occipital, temporal-lateral anterior, temporal-lateral posterior and temporal-mesial.

All clusters containing more than 50 adjacent pixels with a z score > 2 were then identified, and the cluster containing the maximum z score was selected and attributed to one of the predefined ROIs. If this cluster contained pixels of 2 or more ROIs, the center of gravity of the cluster was identified using an automated routine that has been previously validated (*26*). The focus was assumed to be located in the ROI containing the center of gravity of this cluster. Total processing time of this automated program was less than 90 min per patient.

Visual Definition of Lesion

For visual identification of abnormalities suggestive of an epileptogenic lesion, two blinded experienced observers and two blinded less experienced observers analyzed the PET data in standard axial, sagittal and coronal views. To obtain a reliable comparison between the observers and the automated procedure, the suspected lesions were assigned by the observers to 1 of the ROIs dividing the cerebral lobes into sectors that were used for the automated procedure (*25*) (Fig. 1). If multiple abnormalities were detectable, observers selected the suspected focus by following subjective criteria, such as size or intensity of the hypometabolic areas.

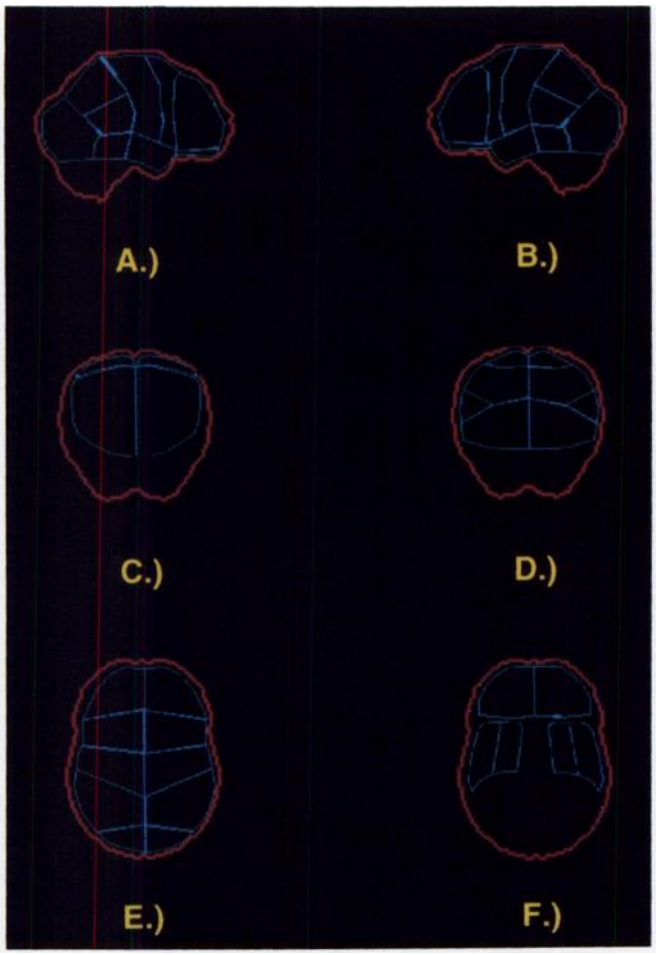

FIGURE 1. Twenty predefined anatomic ROIs placed on surface-projected z score images. Views: right lateral (A), left lateral (B), anterior (C), posterior (D), superior (E) and inferior (F).

Statistical Analysis

For interobserver comparison and comparison of three-dimensional SSP with the visual analyses, a κ test and a Cochran Q test were used. $P = 0.05$ was considered significant.

Noninvasive Methods Used to Identify Seizure Origin

EEG and Seizure Semiology. All patients underwent continuous interictal and ictal EEG video monitoring of several habitual seizures. Ictal and interictal EEG recordings (32–64 channel, Vangard Systems, Cleveland, OH) were obtained in all patients, using closely spaced scalp gold disks, sphenoidal electrodes, the 10/20 system of electrode placement and additional 10/10 electrodes according to the guidelines for a standard electrode position nomenclature of the American Electroencephalographic Society (*27*). The EEG was digitized at a sampling rate of 200 Hz (12 bit), amplified and stored for further analysis.

Seizures were analyzed according to a new classification (*16,17*) with special regard to the possible localization of the seizure onset. In all patients with extratemporal epilepsy and in 2 patients with temporal epilepsy undergoing surgical treatment, additional invasive EEG videos using subdural electrodes (Adtech, Racine, WI) and a digital EEG system (NeuroScan; NeuroSoft, Herndon, VA) were recorded preoperatively. All seizures were analyzed on video and EEG and classified according to the seizure and EEG classification by Luders and Noachtar (*16,17*).

MRI, Ictal [^{99m}Tc]ECD SPECT and Interictal [^{11}C]FMZ PET. High-resolution cerebral MRI studies in axial, sagittal and coronal planes were performed in all patients (1.5-T Magnetom Vision; Siemens, Erlangen, Germany). Images included T1, T2 and proton-density weighted techniques. In patients showing no abnormalities, additional sequences were used (magnetization-prepared rapid gradient echo, fluid-attenuated inversion recovery, three-dimensional fast low-angle shot and ultra-high-resolution MRI with two dual-phase array coils).

For comparison between PET and MRI, an overlay of the nonstereotactically normalized ^{18}F-FDG PET dataset and the T1-weighted MR image was obtained using an interactive tool for image coregistration (*28*). This procedure allowed the accurate identification of the anatomic structure corresponding to the abnormality detected by three-dimensional SSP.

To obtain additional information regarding the focus localization (see Patient Characteristics), ictal SPECT studies with [^{99m}Tc]ECD (*29*) or interictal PET studies with [^{11}C]FMZ were performed (*30*).

RESULTS

Temporal Epilepsy

Preoperative Diagnosis, Postoperative Outcome, Cause and Localization. Of the 27 patients with temporal epilepsy, 23 patients showed clear postoperative improvement (Engel class I or II). Nine of these patients were classified as Engel class Ia, 3 as Ib, 3 as Ic, 4 as Id, 2 as IIa and 2 as IId. Of the 4 patients who had little or no benefit from surgery, 3 were classified as Engel class IIIa and one as IVb.

In the 23 patients who showed significant improvement postoperatively, histopathologic analysis of the resected brain tissue yielded hippocampal scleroses in 20 patients, 2 hamartomas and 1 cavernoma. In the 4 patients who showed no improvement, 1 was found to have gliosis of the resected temporal lobe in addition to a known hypothalamic astrocytoma, and 3 patients were found to have hippocampal sclerosis.

The subsequent sensitivity analysis was performed on the basis of the 23 patients who were classified as Engel class I or II (see Materials and Methods). In this patient group, localization by ictal EEG was consistent with the location of the focus defined by histopathologic criteria. The location within the temporal lobe is summarized in Table 1.

Sensitivity. In 19 of the 23 patients (86%) who improved significantly postoperatively (Engel class I or II), the three-dimensional-SSP localization of the lesion in ^{18}F-FDG PET was consistent with the area of resection.

Experienced observers found a lesion corresponding to the region of resection in 19 of the 23 patients (86%, observer 1) and in 20 of 23 (90%, observer 2), and the less experienced observers found a corresponding lesion in 19 of 23 (86%, observer 3) and 17 of 23 patients (77%, observer 4) (Fig. 2).

MRI findings revealed focal abnormalities in 18 of the patients showing improvement (78%), all in concordance with the definite postoperative focus localization. In the 5 patients in whom no lesions suggestive of a focus were detectable by MRI, the correct localization of the epileptogenic focus was found in 2 patients by three-dimensional SSP and all observers and in 1 patient by observers 1, 2 and 3 but not by three-dimensional SSP.

Of the 4 patients who showed no or minor postoperative improvement, the area of resection coincided with three-dimensional SSP, all observers and MRI in 1 patient. In another patient, the area of resection corresponded to the MRI location and in 1 additional patient with the location defined by observer 2. Of the 2 patients with negative MRI findings, 1 showed an abnormality on [^{99m}Tc]ECD SPECT and 1 on [^{11}C]FMZ PET, both at a localization corresponding to the EEG.

Observer Agreement. Visual definition of the epileptogenic focus generally showed moderate agreement with the localization found by three-dimensional SSP in patients with temporal epilepsy.

Kappa analysis revealed similar agreement between three-dimensional SSP and the experienced observers (κ value: observer 1, 0.39; observer 2, 0.41) as with the less experienced observers (κ value: observer 3, 0.39; observer 4, 0.39). Agreement between experienced observers was good ($\kappa = 0.62$) and moderate between less experienced observers ($\kappa = 0.49$).

TABLE 1
Localization of Focus in Temporal Epilepsy (n = 23)

Temporal lobe	Left	Right	All
Mesial	14	6	20
Lateral	1	2	3
All	15	8	23

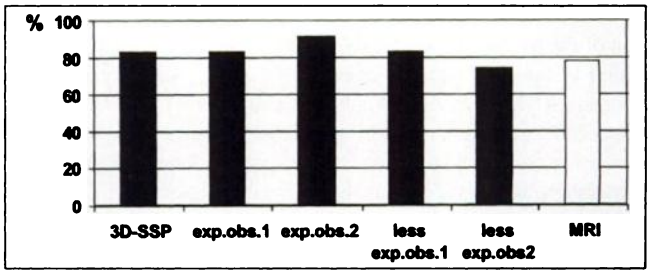

FIGURE 2. Sensitivity of three-dimensional SSP and of observers for detection of epileptogenic focus in temporal epilepsy patients (n = 23) compared with MRI.

The Cochran Q test showed no significant difference between the results of three-dimensional SSP and the observers. A significant difference was found only when comparing the results of observer 2 with those of observer 4 ($P < 0.05$).

Multiple Lesions on Three-Dimensional SSP and MRI. Three-dimensional SSP showed multiple lesions (minimum 50 pixels of a z score > 2) in 11 of the 27 (40%) patients with temporal epilepsy. In 8 of these patients, the automatically selected lesion with the maximum SD was localized in concordance with the actual focus. Of the 3 patients with lesions that were not localized correctly, 2 showed the cluster with the highest maximum in the contralateral temporal lobe and 1 in the ipsilateral parietal lobe. For 2 of these patients, the cluster with the second highest maximum was localized in correspondence with the actual focus.

Compared with three-dimensional SSP, the four observers generally described multiple foci less frequently. MRI showed multiple lesions in 2 patients with temporal epilepsy. Both patients had hippocampal sclerosis in the left temporal lobe; 1 had an additional arachnoidal cyst in the left parietal lobe, and the other had a venous malformation of the left frontal lobe. These abnormalities corresponded to hypometabolic areas detected by three-dimensional SSP and all observers. In the first patient, this morphologic abnormality resulted in mislocalization of the focus by all observers and three-dimensional SSP, whereas in the second, the correct localization could be determined by all observers and three-dimensional SSP.

Extratemporal Epilepsy

Preoperative Diagnosis, Postoperative Outcome, Cause and Localization. Of the 7 patients who underwent epilepsy surgery, 5 were classified as Engel class Ia and 1 patient as IVa.

The follow-up of the remaining patient, who improved postoperatively (see Case Study) was not long enough to allow definite classification. Histopathologic analysis of the resected brain material of the 6 improved patients revealed 4 with cortical dysplasia and 2 with cavernomas. In the patient who did not improve, a cerebral abscess was found.

In 14 of the patients who did not undergo surgery, the information from history, semiology and typical abnormalities on MRI allowed a clear definition of cause. This synoptical diagnosis revealed cortical dysplasia in 5 patients and cavernomas in 2 patients. Furthermore, 1 case of postencephalitic and 1 of post-traumatic epilepsy, 1 brain abscess, 2 tumors, 1 schizencephaly and 1 perinatal infarction were diagnosed.

MRI showed focal irregularities in 11 of the 15 patients with extratemporal epilepsy who did not undergo surgery. In 9 of those patients, the MRI abnormalities were localized in correspondence with the EEG localization. The other 2 showed a hypothalamic hamartoma and a vascular malformation, both in discordance with the EEG localization. Of these 2 patients, 1 showed a lesion on [^{11}C]FMZ PET and 1 on [^{11}C]FMZ PET and ictal [^{99m}Tc]ECD SPECT concordant with the EEG. Of the remaining 4 patients with no apparent abnormalities on high-resolution MRI, 1 showed an abnormality on [^{11}C]FMZ PET and 3 on both [^{11}C]FMZ PET and ictal [^{99m}Tc]ECD SPECT in a localization corresponding to ictal EEG and seizure semiology.

The location of the epileptogenic area defined by the methods described above is summarized in Table 2.

Sensitivity. All patients with extratemporal epilepsy were included in the sensitivity analysis, with the exception of the patient who did not improve significantly after surgery.

In 14 of the 21 included patients (67%), three-dimensional SSP enabled an accurate localization of the epileptogenic focus compared with the predefined localization. Experienced observers detected the focus in 8 (38%, observer 1) and 7 patients (33% observer 2). Less experienced observers localized the focus correctly in only 4 patients (19%, both observers). MRI was able to localize the focus correctly in 12 of the 21 patients with extratemporal epilepsy (57%, Fig. 3).

MRI showed no abnormalities in 7 patients, and in 2 other patients the MRI abnormalities described did not correspond with the final focus localization. In these 9 patients, a correct localization was found by three-dimensional SSP in 6 patients and by observers in 3 patients by some and 4 by others.

Regarding selectively the patients who underwent surgery, ictal EEG was consistent with the focus defined by histopathologic criteria in all patients with postoperative improvement. In 3 of the 6 patients who improved postoperatively, MRI showed a lesion corresponding in localization

TABLE 2
Localization of Focus in Extratemporal Epilepsy (n = 21)

Lobe	Left	Right	All
Frontal	2	11	13
Central	3	1	4
Parietal	1	1	2
Occipital	0	2	2
All	6	15	21

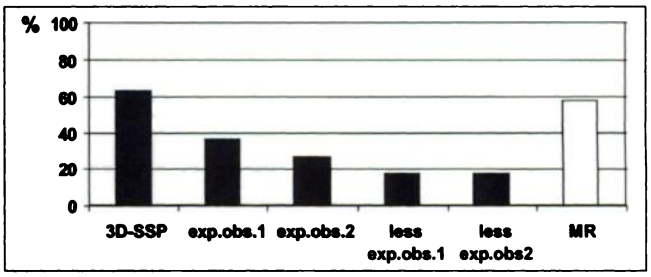

FIGURE 3. Sensitivity of three-dimensional SSP and of observers for detection of epileptogenic focus in extratemporal epilepsy patients (n = 21) compared with MRI.

with the resected region. Localization was defined accurately by three-dimensional SSP in 5 patients, by observer 1 in 3, by observer 2 in 1 and by each less experienced observer in 1 of the 6 improved patients. In the 1 patient who showed no postoperative improvement (Engel class IVa), the epileptogenic lesion had been determined in correspondence with the ictal EEG by MRI, three-dimensional SSP and by all observers.

Observer Agreement. Visual analysis generally showed weak agreement with the localization found by three-dimensional SSP in extratemporal patients. Kappa-analysis revealed better agreement of three-dimensional SSP with the experienced observers (κ value: observer 1, 0.32; observer 2, 0.35) than with the less experienced observers (κ value: observer 3, 0.17; observer 4, 0.23). Agreement between experienced observers was good ($\kappa = 0.58$) but weak between less experienced observers ($\kappa = 0.38$).

The Cochran Q test revealed a significant difference between the results of three-dimensional SSP compared with all observers ($P < 0.05$). In addition, there was a significant difference between observer 1 and observer 4 ($P < 0.05$).

Multiple Lesions on Three Dimesional SSP and MRI. Three-dimensional SSP showed multiple lesions (minimum 50 pixels of a z score > 2) in 17 of the 22 (77%) patients with extratemporal epilepsy. Using the algorithm described above, a correct localization was possible in 12 of the 17 patients. In the other 5 patients, the highest maximum was localized in the temporal lobe ipsilateral to the actual focus in 3 patients, in the occipital lobe in 1 and in the frontal lobe in 1 patient, both contralateral to the actual focus. The second highest maximum represented the correct focus localization in 2 of these patients.

As in temporal epilepsy, observers found multiple lesions less frequently than three-dimensional SSP. However, altogether more cases of multiple lesions were found in extratemporal epilepsy by observers and three-dimensional SSP compared with temporal epilepsy. MRI showed multiple lesions in 4 patients with extratemporal epilepsy (18%). In these patients, the definition of the final focus localization was based on correspondence with other methods (EEG, [^{11}C]FMZ PET and ictal [^{99m}Tc]ECD SPECT]). The multiple lesions in these 4 patients were all detected on PET imaging by three-dimensional SSP. Table 3 summarizes the fre-

TABLE 3
Frequency of Detection of Multiple Lesions by Different Observers/3D-SSP/MRI

Multiple lesions	3D-SSP	Experienced observers		Less experienced observers		MRI
		1	2	3	4	
Temporal (n = 27)	11 (40%)	5 (19%)	5 (19%)	6 (22%)	7 (26%)	2 (9%)
Correct lesions selected	8	4	4	4	2	
Extratemporal (n = 22)	17 (77%)	9 (41%)	12 (55%)	8 (36%)	9 (41%)	4 (18%)
Correct lesions selected	12	2	4	2	2	

3D-SSP = three-dimensional stereotactic surface projection.

quency of multiple lesions and the correct focus selection with three-dimensional SSP and by the different observers compared with MRI for temporal and extratemporal epilepsy.

Case Study

An 18-y-old woman suffered from seizures since the age of 3. Seizures started as tonic spasms of the face, extremities and the neck and subsequently changed into a clonic seizure of the left arm and the head and then into a versive seizure of the left side of the head. The patient reported occasional, generalized seizures. Continuous EEG showed intermittent slowing, interictal spikes and ictal seizure onset in the right frontal lobe in paramedian location corresponding to the supplementary motor area (SMA) (Fig. 4D). These findings were confirmed by invasive EEG with subdural electrodes. High-resolution MRI and [^{11}C]FMZ PET showed no abnormalities (Figs. 4C, 5A and 5D). Ictal [^{99m}Tc]ECD SPECT showed diffusely enhanced regional cerebral blood flow in the mesial and lateral premotor to prefrontal cortex of the right side.

Subsequently, a resection of the right superior and medial frontal gyrus anterior to the precentral gyrus was performed. The histopatholgical analysis revealed a small dysplasia as the cause of the disease. Postoperatively, the patient has been seizure free (8 wk), but due to the short postoperative interval no definite classification of the postoperative outcome according to the Engel criteria is possible.

Figure 3 shows three-dimensional SSP images after stereotactic surface mapping and a z score image resulting from the comparison with the normal database. The superior view (Fig. 4A) shows a small hypometabolic area in the right paramedian frontal lobe corresponding to the SMA. In the z score image (Fig. 4B), the lesion is more clearly visible. This paramedian frontal area contains the highest maximum in the z score image, i.e., the highest deviation from the normal control population. The ictal onset in the EEG (Fig. 4D, superior view) at a right paramedian prefrontal localization corresponds exactly with the automatically defined abnormality on ^{18}F-FDG PET. Figure 4C is the [^{11}C]FMZ PET scan of the patient, which showed no abnormalities. Because of the nonlinear warping procedure, the lesion shown on the surface images does not represent the exact localization on the patient's brain. For this reason, an overlay of the original PET scan on the individual MR image was performed. After detection of the lesion on the surface images and attachment to a circumscript brain region, identification in the original slice display is easily possible. An overlay of the transversal and sagittal slices with the individual MR image was generated to identify the corresponding localization on the MR image, on which no abnormality was apparent (Figs. 5C and 5F). Compared with the three-dimensional SSP surface-rendered images and the three-dimensional SSP z score images, the subtle character of the changes in the slice display is apparent. Visual

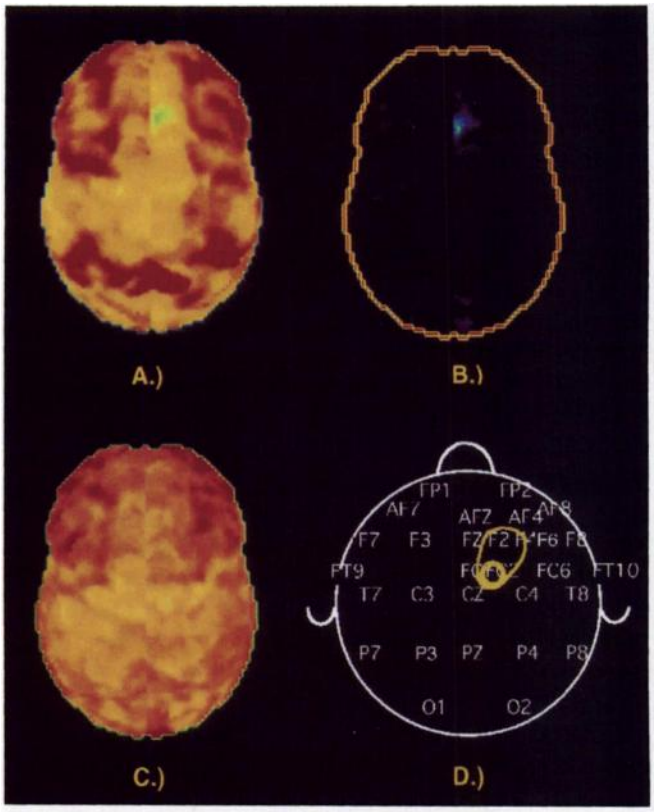

FIGURE 4. Case study. (A) Superior view on surface-projected ^{18}F-FDG PET image. (B) Corresponding z score image. (C) Corresponding [^{11}C]FMZ image of 18-y-old woman. (D) Seizure onset during EEG.

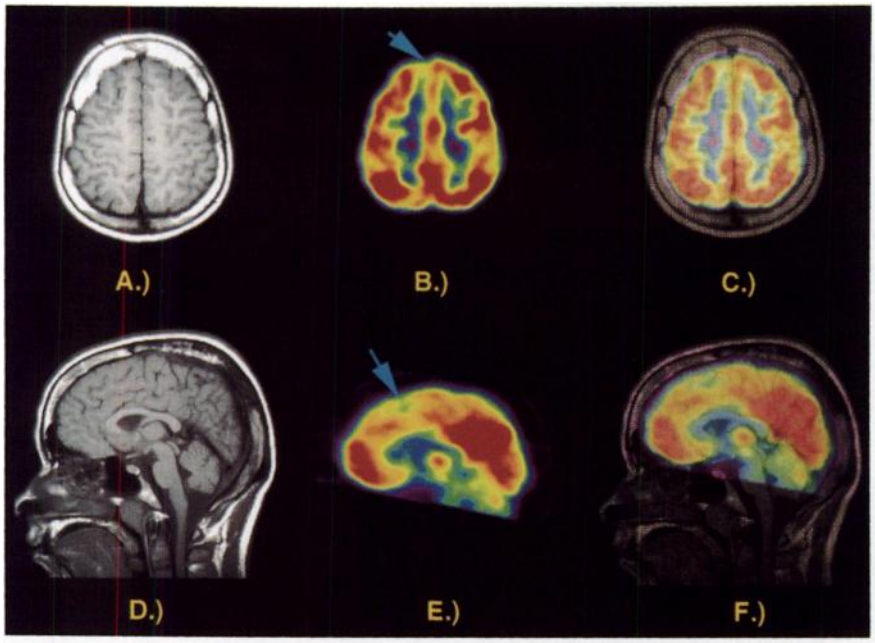

FIGURE 5. Case study. (A and D) Individual MR images. (B and E) ^{18}F-FDG PET (arrow pointing at hypometabolic area). (C and F) Overlay. A–C show inferior views on axial slices. D–F show medial views on sagittal slices.

analysis by two experienced and two less experienced observers using transaxial, sagittal and coronal slices did not lead to correct localization of the lesion. The exact identification of the epileptogenic focus with ^{18}F-FDG PET was of particular interest in this patient, because neither MRI nor [^{11}C]FMZ PET showed specific abnormalities.

DISCUSSION

In this study, a fully automated observer-independent analytic approach (three-dimensional SSP), previously evaluated for the identification of abnormalities in dementing disorders (*8,15*), was applied for the first time to the analysis of PET studies in patients with focal epilepsy. In addition to patients with temporal epilepsy, the patient population included a comparatively large group with extratemporal seizure origin, a population in which the overall sensitivity of PET is known to be unsatisfactorily low (*3,5,6*). An improvement of diagnostic accuracy is, therefore, of special relevance for this population. To increase the number of patients with extratemporal epilepsy for this study, patients were added in whom noninvasive diagnostic procedures localized the epileptogenic area with high confidence. However, whenever possible, focus localization was confirmed by surgical treatment.

In the temporal epilepsy group, there was no clear improvement in the diagnostic accuracy of three-dimensional SSP compared with visual analysis. In this selected patient sample, the sensitivity of the visual analysis (86%–90%) and of three-dimensional SSP (86%) was consistent with previously published results of larger populations of epilepsy patients (*2–3,14,18*). Postoperative outcome in this population was good considering international standards (*4*).

In the clinical setting, three-dimensional SSP did not add additional information for the correct lateralization of the temporal focus in patients with suspected temporal lobe epilepsy compared with visual and semiquantitative analysis with ROIs. However, the program provided sufficient information to exclude other extratemporal abnormalities.

In addition, it is important to note that in 3 of 4 patients with temporal epilepsy who did not improve significantly, surgical resection was performed in a region that did not correspond with the three-dimensional SSP localization. One of these patients had, in addition to the temporal gliosis where the resection was performed, a hypothalamic astrocytoma corresponding to the area with the highest abnormality on three-dimensional SSP. Because seizures continued after temporal lobe resection, a possible explanation could be that the astrocytoma was the actual seizure origin. Ictal EEG, however, localized the seizure onset in the temporal region. In another of these patients, localization of ictal spikes by EEG was not possible until 29 s after seizure onset and thus, might not have localized the seizure origin sufficiently. This patient continued to have ictal patterns on EEG localized in the temporal region after anterior temporal lobe resection. Perhaps the epileptogenic tissue in this patient was disseminated throughout wider parts of the temporal lobe and, therefore, the anterior resection was not sufficient. The 2 other patients showed no conspicuous irregularities in their history or in their pre- and postoperative findings. The limited number and the heterogeneity of the patients do not justify speculations about the relationship between patient outcome and the localization of the hypometabolic lesions determined by three-dimensional SSP.

In the extratemporal epilepsy group, this observer-independent approach localized the epileptogenic area correctly significantly more often than the visual observer approach. The sensitivity of the visual assessment, at least of the experienced observers (33%–38%), was comparable

with data published by other groups reporting their results of nonselected populations (*3,5,6*). The sensitivity of three-dimensional SSP, therefore, was higher than in most other studies reporting on comparable patient populations (*3,5,6*). Using this observer-independent analysis clinically is helpful in reducing observer variability. Specifically, it can improve the quality of rating of inexperienced readers. In addition to the higher sensitivity in the clinical setting, this approach has been shown to be beneficial because it allows fast detection of abnormalities, which can then be identified on the conventional slice display needed for the overlay with the MR image for preoperative planning, as demonstrated in the case study. Although only a minority of patients in this group underwent surgical therapy, the agreement between the results of three-dimensional SSP and the final localization of the epileptogenic lesion indicates a high diagnostic accuracy.

Because of the design of the study, specificity could not be determined. This is also true for the MRI results reported in this study. Positive MRI was an inclusion criterion for the patients, and therefore, the high number of correctly positive MRI studies (78% for temporal and 57% for extratemporal) can be expected. These figures are indeed higher than the results reported from unselected samples (*3*). It is, therefore, remarkable that three-dimensional SSP correctly localized the lesion in 6 patients in the extratemporal group, with MRI being negative or incorrect even in high-resolution technique, as demonstrated in the case study. Three of these lesions were not detected by any of the observers.

In both the temporal and the extratemporal epilepsy groups, the three-dimensional SSP analysis detected multiple abnormalities in more cases than the observers and MRI. The overall number was lower in the temporal group, which is consistent with previously reported results (*5*). However, the lesions detected by this approach do not represent an actual abnormality of cerebral glucose metabolism in all cases. In some cases, anatomic variabilities, such as wide sulci, led to inaccuracies in the stereotactic normalization, yielding small areas with high values in the z score image (*8*). The selection of clusters of pixels of a sufficient size should have minimized misinterpretations of these areas. Furthermore, the visual comparison with the nonnormalized images in the slice display would make such artificial lesions apparent, especially when overlaid on the individual MR images.

By selection of the highest deviation from the reference database, three-dimensional SSP had a significantly higher sensitivity in the extratemporal group and a higher accuracy compared with the observers, who used subjective criteria for selection among multiple lesions. However, it has to be taken critically into consideration that although only patients with extratemporal epilepsy with high probability for a single focus were included in the study, the presence of multiple foci cannot be completely excluded in the subgroup that did not undergo surgical therapy and may represent a more widespread distribution of epileptogenic brain tissue. This has also been suspected previously to render EEG localization difficult in these cases (*9*).

Multifocal epilepsy can be ruled out for the temporal group, in which the successful resection provided evidence for a single epileptogenic area.

Several approaches have been used for the quantitative analysis of ^{18}F-FDG PET images in epilepsy (*31–35*). The vast majority evaluated in patients with epilepsy were based on ROIs. Basically, two kinds of ROI structures were used for quantitative analysis of PET data in most of these studies: (a) predetermined geometric configurations (circles or squares) and (b) irregular shapes formed to fit the margins of the subdivisions of the images (*13*). The visual placement of geometrical ROIs is currently the most widely used method (*10,31,33,34*). Absolute measurement of the regional metabolic rate of glucose and relative quantification using values such as the asymmetry index have been applied (*34,36*). Compared with the analytic method used in this study (three-dimensional SSP), these approaches have several disadvantages. The visual placement of ROIs is highly subjective and has poor reproducibility. Furthermore, contralateral lesions might lead to false-negative results, especially in semiquantitative approaches. The use of ROIs in selected slices and selected regions is sufficient for the detection of foci in typical localization, e.g., in mesial temporal lobe epilepsy, but will most probably miss circumscript foci in atypical regions (such as in the orbitofrontal cortex or near the corpus callosum), as was shown for the SMA in the case study. To avoid this, one has to cover the entire brain with ROIs. Swartz et al. (*34*) achieved improved sensitivity of ^{18}F-FDG PET in extratemporal epilepsy patients with such an approach. In their study, 87 individualized ROIs were manually drawn in every dataset, covering all gray matter areas. Although the sensitivity of this method is relatively high, it is time consuming and requires a person experienced in this procedure. In contrast, three-dimensional SSP reveals similar results but requires user interaction for less than 15 min. Therefore, it appears to be much more suitable in a routine clinical setting.

Although three-dimensional SSP has no advantages for correct lateralization of the epileptogenic focus over simple ROI-based analysis in patients with temporal epilepsy, the comparison with a normal database can be helpful for patients with bilateral abnormalities. Furthermore, as mentioned above, additional extratemporal foci can be easily detected because the entire brain is visualized in surface projections.

There are several methods using a three-dimensional display of the brain surface, for example, the one proposed by Hashikawa et al. (*37*). However, without stereotactic normalization, no direct comparison with a normal database is possible, allowing only visual assessment and no observer-independent quantification of abnormalities. A disadvantage of stereotactic normalization is that because of the nonlinear warping procedure, the localization of the epileptogenic focus on the surface map does not represent the actual

localization on the individual brain; it only illustrates the localization on a standardized brain surface. Thus, for the further preparation of surgical therapy, e.g., the placement of invasive EEG electrodes, it is necessary to identify the abnormality detected in the statistical comparison in the nondeformed individual images, which then can be overlaid on the MR image to allow accurate anatomic identification of localization and extent of the functional abnormalities. However, as illustrated in the case study, this is easily done and cannot be regarded as a serious limitation of the application of three-dimensional SSP in this setting.

Other software packages based on stereotactic normalization and pixelwise comparison of different datasets such as statistical parametric mapping (SPM) (*38*) can also be adapted to allow comparison of patients with a normal database and a surface display of the results similar to three-dimensional SSP. However, these packages have never been systematically tested for their reliability in analyzing clinical ^{18}F-FDG PET studies during preoperative evaluation of focal epilepsy. Richardson et al. (*39*) and Koepp et al. (*40*) have used SPM in scientific studies with [^{11}C]FMZ in epilepsy patients for the comparison of abnormalities in benzodiazepine receptor binding with a normal database. The goal of these studies, however, was not to determine the diagnostic accuracy of this approach, and they did not report surgical results in the patients with extratemporal epilepsy. Therefore, it is not possible to deduce from these results the usefulness of this analytical package for the analysis of ^{18}F-FDG PET studies of epilepsy patients. Differences in the algorithms used for stereotactic normalization and statistical comparison between three-dimensional SSP, SPM and other programs originally developed for PET activation studies require a separate evaluation for every software package.

Although the patient population evaluated was limited, this study has demonstrated that these statistical approaches are generally suitable for the clinical routine analysis of PET studies of epilepsy patients and can be especially helpful for the detection of extratemporal foci.

CONCLUSION

In this study, it was shown that the automated observer-independent three-dimensional SSP routine increases sensitivity and reduces observer variability of the analysis of ^{18}F-FDG PET images in patients with extratemporal epilepsy and is, therefore, a useful tool in the evaluation of this patient group. In patients with temporal epilepsy the benefit is less apparent, but the routine proved to be valuable for the exclusion of additional extratemporal foci.

ACKNOWLEDGMENTS

We thank Brigitte Dzewas, Coletta Kruschke and Claudia Kolligs for their technical assistance and the radiochemistry group for their reliable supply of radiopharmaceuticals. We are obliged to Jodi Neverve for the careful review of the manuscript. We also thank Raymonde Busch, Department of Medical Statistics and Epidemiology, Technische Universität, München, for her advice and support in the statistical analysis.

REFERENCES

1. Kuhl DE, Engel J Jr, Phelps ME, Kowell AP. Epileptic patterns of local cerebral metabolism and perfusion in man: investigation by emission computed tomography of ^{18}F-fluorodeoxyglucose and ^{13}N-ammonia. *Trans Am Neurol Assoc.* 1978;103:52–53.
2. Henry TR, Engel J Jr, Mazziotta JC. Clinical evaluation of interictal fluorine-18-fluorodeoxyglucose PET in partial epilepsy. *J Nucl Med.* 1993;34:1892–1898.
3. Spencer SS. The relative contributions of MRI SPECT and PET imaging in epilepsy. *Epilepsia.* 1994;35(suppl 6):S72–S89.
4. Engel J Jr. Update on surgical treatment of the epilepsies. Summary of the Second International Palm Desert Conference on the Surgical Treatment of the Epilepsies (1992). *Neurology.* 1993;43:1612–1617.
5. Engel J Jr, Henry TR, Swartz BE. Positron emission tomography in frontal lobe epilepsy. *Adv Neurol.* 1995;66:223–238.
6. Henry TR, Sutherling WW, Engel J Jr, et al. Interictal cerebral metabolism in partial epilepsies of neocortical origin. *Epilepsy Res.* 1991;10:174–182.
7. Engel J Jr. *Seizures and Epilepsy.* Philadelphia, PA: FA Davis; 1989.
8. Bartenstein P, Minoshima S, Hirsch C, et al. Quantitative assessment of cerebral blood flow in patients with Alzheimer's disease by SPECT *J Nucl Med.* 1997;38:1095–1101.
9. Quesney LF, Constain M, Rasmussen T, Olivier A, Palmini A. Presurgical EEG investigation in frontal lobe epilepsy. *Epilepsy Res.* 1992;5(suppl):55–69.
10. Henry TR, Mazziotta JC, Engel J Jr. The functional anatomy of frontal lobe epilepsy studied with PET. *Adv Neurol.* 1992;57:449–463.
11. Sveinbjornsdottir S, Duncan JS. Parietal and occipital lobe epilepsy: a review. *Epilepsia.* 1993;34:493–521.
12. Engel J Jr. PET scanning in partial epilepsy. *Can J Neurol Sci.* 1991;18:588–592.
13. Williamson PD, Thadani VM, Darcey TM, Spencer DD, Spencer SS, Mattson RH. Occipital lobe epilepsy: clinical characteristics seizure spread patterns and results of surgery. *Ann Neurol.* 1992;31:3–13.
14. Duncan JS. Imaging and epilepsy. *Brain.* 1997;120:339–377.
15. Minoshima S, Frey KA, Koeppe RA, Foster NL, Kuhl DE. A diagnostic approach in Alzheimer's disease using three-dimensional stereotactic surface projections of fluorine-18-FDG-PET. *J Nucl Med.* 1995;36:1238–1248.
16. Noachtar S, Luders HO. Classification of epileptic seizures and epileptic syndromes. In: Gildenberg PL, Taxer RR, eds. *Textbook of Stereotactic and Functional Neurosurgery.* New York, NY: McGraw-Hill; 1997:1763–1775.
17. Luders HO, Noachtar S. *Atlas und Video Epileptischer Anfälle und Syndrome.* Wehr Baden, Germany: Ciba Geigy; 1995.
18. Engel J Jr. Clinical neurophysiology neuroimaging and the surgical treatment of epilepsy. *Curr Opin Neurol Neurosurg.* 1993;6:240–249.
19. Minoshima S, Berger KL, Lee KS, Mintun MA. An automated method for rotational correction and centering of three-dimensional functional brain images. *J Nucl Med.* 1992;33:1579–1585.
20. Minoshima S, Koeppe RA, Frey KA, Ishihara M, Kuhl DE. Stereotactic PET atlas of the human brain: aid for visual interpretation of functional brain images. *J Nucl Med.* 1994;35:949–954.
21. Minoshima S, Koeppe RA, Frey KA, Kuhl DE. Anatomic standardization: linear scaling and nonlinear warping of functional brain images. *J Nucl Med.* 1994;35: 1528–1537.
22. Minoshima S, Giordani B, Berent S, Frey KA, Foster NL, Kuhl DE. Metabolic reduction in the posterior cingulate cortex in very early Alzheimer's disease. *Ann Neurol.* 1997;42:85–94.
23. Talairach J, Tournoux P. *Co-Planar Stereotaxic Atlas of the Human Brain.* New York, NY: Thieme; 1988.
24. Arnold S, Schlaugg G, Niemann H, et al. Topography of interictal glucose hypometabolism in unilateral mesiotemporal epilepsy. *Neurology.* 1996;46:1422–1430.
25. Damasio AR, Damasio H, Christen Y. *Neurobiology of Decision-Making.* Berlin, Germany: Springer-Verlag; 1996.
26. Weber W, Bartenstein P, Gross M, et al. Fluorine-18-FDG PET and iodine-123-IMT SPECT in the evaluation of brain tumors. *J Nucl Med.* 1997;38:802–808.
27. American Electroencephalographic Society. Guidelines for a standard electrode position nomenclature. *J Clin Neurophysiol.* 1991;8:200–202.
28. Pietrzyk U, Herholz K, Fink G, et al. An interactive technique for three-dimensional image registration: validation for PET SPECT MRI and CT brain studies. *J Nucl Med.* 1994;35:2011–2018.
29. Noachtar S, Arnold S, Yousry TA, et al. Ictal technetium-99m ethyl cysteinate dimer single-photon emission tomographic findings and propagation of epileptic

seizure activity in patients with extratemporal epilepsies. *Eur J Nucl Med.* 1998;25:166–172.
30. Koeppe RA, Holthoff VA, Frey KA, Kilbourn MR, Kuhl DE. Compartmental analysis of [^{11}C]flumazenil kinetics for the estimation of ligand transport rate and receptor distribution using positron emission tomography. *J Cereb Blood Flow Metab.* 1991;11:735–744.
31. Breier JI, Mullani BA, Thomas AB, et al. Effects of duration of epilepsy on the uncoupling of metabolism and blood flow in complex partial seizures. *Neurology.* 1997;48:1047–1053.
32. Theodore WH, Newark ME, Sato S, et al. [F-18]-fluordeoxyglucose positron emission tomography in refractory complex partial seizures. *Ann Neurol.* 1983;14: 429–437.
33. Henry TR, Mazziotta JC, Engel J Jr, et al. Quantifying interictal metabolic activity in human temporal lobe epilepsy. *J Cereb Blood Flow Metab.* 1990;10:748–757.
34. Swartz BE, Khonsari A, Brown C, Mandelkern M, Simpkins F, Krisdakumtorn T. Improved sensitivity of [F-18]-FDG-positron emission tomography scans in frontal and "frontal plus" epilepsy. *Epilepsia.* 1995;36:388–395.
35. Fox PT, Perlmutter JS, Raichle ME. A stereotactic method of anatomical localization for positron emission tomography. *J Comput Assist Tomogr.* 1985;9:141–153.
36. Gur RC, Gur RE, Sussman NM, Selzer ME. Positron emission tomography in epilepsy. In: Reivitch M, Alavi A, eds. *Positron Emission Tomography.* New York, NY: Alan R. Liss; 1985:263–271.
37. Hashikawa K, Matsumoto M, Moriwaki H, et al. Three-dimensional display of surface cortical perfusion by SPECT: application in assessing Alzheimer's disease. *J Nucl Med.* 1995;36:690–696.
38. Friston KJ, Frith CD, Liddle PF, Frackowiack RSJ. Comparing functional (PET) images: the assessment of significant change. *J Cereb Blood Flow Metab.* 1991;11:690–699.
39. Richardson MP, Koepp MJ, Brooks DJ, Fish DR, Duncan JS. Benzodiazepine receptors in focal epilepsy with cortical dysgenesis: an ^{11}C-flumazenil PET study. *Ann Neurol.* 1996;40:188–198.
40. Koepp MJ, Labbe C, Richardson MP, et al. Regional hippocampal [C-11]flumazenil PET in temporal lobe epilepsy with unilateral and bilateral hippocampal sclerosis. *Brain.* 1997;120:1865–1876.